FULL PAPER

BJC

British Journal of Cancer (2015) 112, 693–703 | doi: 10.1038/bjc.2015.16

Keywords: Paediatric high grade glioma; DIPG; migration; lithium; indirubin

Cell migration in paediatric glioma; characterisation and potential therapeutic targeting

J V Cockle*[,1,2], S Picton[2], J Levesley[1], E Ilett[1], A M Carcaboso[3], S Short[1], L P Steel[1], A Melcher[1], S E Lawler[4] and A Brüning-Richardson[1]

[1]Leeds Institute of Cancer Studies and Pathology, University of Leeds, Wellcome Trust Brenner Building, St James's University Hospital, Leeds, LS9 7TF, UK; [2]Yorkshire Regional Centre for Paediatric Oncology and Haematology, Leeds General Infirmary, Great George Street, Leeds, LS1 3EX, UK; [3]Preclinical Therapeutics and Drug Delivery Research Program, Department of Oncology, Hospital Sant Joan de Déu Barcelona, Preclinical Therapeutics and Drug Delivery Research Program Santa Rosa, 39-57, 4th floor 08950 Esplugues de Llobregat, Barcelona, Spain and [4]Department of Neurosurgery, Brigham and Women's Hospital, Harvard Medical School, 4 Blackfan Circle, HIM 930A, Boston, MA, 02115, USA

Background: Paediatric high grade glioma (pHGG) and diffuse intrinsic pontine glioma (DIPG) are highly aggressive brain tumours. Their invasive phenotype contributes to their limited therapeutic response, and novel treatments that block brain tumour invasion are needed.

Methods: Here, we examine the migratory characteristics and treatment effect of small molecule glycogen synthase kinase-3 inhibitors, lithium chloride (LiCl) and the indirubin derivative 6-bromoindirubin-oxime (BIO), previously shown to inhibit the migration of adult glioma cells, on two pHGG cell lines (SF188 and KNS42) and one patient-derived DIPG line (HSJD-DIPG-007) using 2D (transwell membrane, immunofluorescence, live cell imaging) and 3D (migration on nanofibre plates and spheroid invasion in collagen) assays.

Results: All lines were migratory, but there were differences in morphology and migration rates. Both LiCl and BIO reduced migration and instigated cytoskeletal rearrangement of stress fibres and focal adhesions when viewed by immunofluorescence. In the presence of drugs, loss of polarity and differences in cellular movement were observed by live cell imaging.

Conclusions: Ours is the first study to demonstrate that it is possible to pharmacologically target migration of paediatric glioma *in vitro* using LiCl and BIO, and we conclude that these agents and their derivatives warrant further preclinical investigation as potential anti-migratory therapeutics for these devastating tumours.

Paediatric high grade glioma (pHGG) and diffuse intrinsic pontine glioma (DIPG) are highly aggressive tumours associated with dismal prognosis. Paediatric high grade gliomas account for 8–12% of all primary paediatric CNS tumours (Jones *et al*, 2012). Current treatment regimens involve maximal surgical resection, radiation therapy and chemotherapy. However, despite this intensive treatment approach, 5-year survival remains between 15 and 35% (Broniscer and Gajjar, 2004). Diffuse intrinsic pontine gliomas are the most common brainstem tumours of childhood and represent one of the most challenging paediatric tumours to treat. Surgery is not an option, chemotherapeutics have failed to improve outcomes, and radiotherapy can only temporarily slow disease progression, which is associated with median survival of less than 1 year (Warren, 2012). Both pHGG and DIPG are known to have diffuse infiltrative growth patterns, and this invasive phenotype contributes to their limited therapeutic response (Demuth and

*Correspondence: Dr JV Cockle; E-mail: j.v.cockle@leeds.ac.uk

Revised 12 December 2014; accepted 17 December 2014; published online 27 January 2015

Berens, 2004; Louis, 2006). As a result, there is a pressing clinical need to develop novel therapeutic approaches that effectively reduce such paediatric brain tumour migration and invasion.

Adult HGG cells are known to migrate in specific patterns, following the orientation of white matter tracts, capillaries and unmyelinated axons (Louis, 2006; Agudelo-Garcia *et al*, 2011). Recent studies have suggested that glycogen synthase kinase-3 (GSK-3), a serine/threonine protein kinase, plays a key role in orchestrating cell migration, through regulating cellular structure, motility and dynamics of the cytoskeleton (Grimes and Jope, 2001; Wakefield *et al*, 2003; Sun *et al*, 2009). The effects of small molecule GSK-3 inhibitors on blocking adult glioma migration and invasion have been demonstrated both *in vitro* and *in vivo* (Nowicki *et al*, 2008; Williams *et al*, 2011) and offer a potential novel anti-invasive approach for glioma. The effects of GSK-3 inhibitors on pHGG and DIPG migration and invasion are unknown, and given the distinct biological and clinical phenotype of the adult and paediatric diseases (Jones *et al*, 2012), warrant separate investigation.

Very few studies have focused on identifying existing or novel therapeutic agents that are capable of impairing migration and invasion in pHGG and DIPG owing to limited patient tissue availability. We have conducted a comprehensive analysis of cell migration in two pHGG cell lines and one rare patient-derived DIPG cell line using a range of 2D and 3D assays. In addition, we also demonstrate for the first time that treatment with the small molecule GSK-3 inhibitors, lithium chloride (LiCl) and the indirubin derivative 6-bromoindirubin-oxime (BIO), which have previously been shown to block migration of adult glioma cells (Nowicki *et al*, 2008; Williams *et al*, 2011), also inhibit the migration of pHGG and DIPG cells *in vitro*. These agents represent novel anti-invasive candidates that may improve the clinical management of these challenging diseases in children.

MATERIALS AND METHODS

Cell lines and reagents. Paediatric glioma cell lines SF188 (Grade IV, Glioblastoma) and KNS42 (Grade IV, Glioblastoma) were obtained from Dr Chris Jones (Institute of Cancer Research, London, UK). Cells were grown in Dulbecco's Modified Eagles' medium (Sigma-Aldrich, Dorset, UK) with 10% heat-inactivated foetal calf serum (Labtech, East Sussex, UK) and 0.5% penicillin-streptomycin (Sigma-Aldrich). Cell line identity was verified by serial tandem repeat profiling at the University of Leeds. The patient autopsy-derived DIPG cell line HSJD-DIPG-007 was obtained from Dr Angel M. Carcaboso (Hospital Sant Joan de Déu Barcelona, Barcelona, Spain). Cells were cultured as tumour spheres in tumour stem base medium (Life Technologies, Paisley, UK) supplemented with B-27 (Life technologies) and human growth factors EGF, FGF-basic, PDGF-AA and PDGF-BB (Peprotech, Rocky Hill, NJ, USA). All cell lines were free of mycoplasma contamination.

Reagents used were LiCl (Sigma-Aldrich) and BIO (Calbiochem, Nottingham, UK).

Three-dimensional cell migration/invasion assay. For three-dimensional spheroid cultures, 1×10^3 cells were incubated for 72 h in an ultra-low attachment round bottom 96-well plate (Costar, Corning Lifesciences, Tewksbury, MA, USA). Aggregates were then encased in 100 μl of rat tail collagen-1 (BD Biosciences) neutralised with 1 M sodium hydroxide (NaOH) in 5 × Dulbecco's Modified Eagles' medium. After polymerisation at 37 °C, the collagen was overlaid with 100 μl of standard growth medium ± GSK-3 inhibitors over a range of concentrations. Spheroid expansion and invasion into the collagen matrix was monitored for 72 h using the EVOS cell imaging system (Advanced Microscopy Group, Life Technologies) and analysed with Volocity 3D Image Analysis software (Perkin-Elmer Inc., Coventry, UK) and Image J (http://rsbweb.nih.gov/ij). In order to quantify migration, two zones of migration were defined: the *invasion zone* represents the area outside the spheroid core to where approximately 75% of migrating cells invaded into, whereas the *leading edge zone* represents the total area containing migrated cells (Supplementary Figure 1). This method has been previously described (Ma *et al*, 2011) and improved the accuracy of the analysis. The migration index was calculated as

$$\frac{\text{area of zone} - \text{area of core}}{\text{total area}}$$

Transwell migration assay. Transwell assays were performed using 8 μm pore inserts (Greiner Bio-One, Stroud, UK) pre-coated with 5 μg ml^{-1} of the chemo-attractant fibronectin (Sigma). Cell lines were pre-treated ± 20 mM LiCl or 5 μM BIO for 1 h. Cells (5×10^4) were then placed into transwell inserts in triplicate and allowed to migrate for 4 h. Migrated cells were fixed with 1% glutaraldehyde (Sigma-Aldrich) in PBS and visualised by staining with 0.1 μg ml^{-1} DAPI (Biotium, Hayward, CA, USA). Migration was determined by imaging DAPI nuclear stain with the EVOS imaging system and quantifying the fluorescence signal for the individual transwells using Volocity 3D Image Analysis software.

Migration on nanofibre scaffolds. To evaluate migration on 3D nanofibre scaffolds, 1×10^3 cells labelled with Cell Tracker Green dye (Invitrogen, Paisley, UK) were cultured as hanging drops as described (Del Duca *et al*, 2004). Spheroid aggregates were transferred into wells of aligned poly-ε-caprolactone nanofibre-coated culture plates (Nanofibre solutions, Columbus, OH, USA), which allows cell migration on a 3D scaffold stimulated by topographical cues (Johnson *et al*, 2009). Spheroids were incubated at 37 °C in growth medium ± 20 mM LiCl or 5 μM BIO in triplicate and migration was monitored for 72 h using the EVOS imaging system and quantified using Image J software.

Immunofluorescence (IF) and western blotting. Antibodies for IF studies were rat anti-alpha tubulin monoclonal antibody (Serotec, Kidlington, UK), rabbit anti-β-catenin antibody (Sigma-Aldrich) and secondary antibodies (Alexa Fluor-conjugated reagents obtained from Molecular Probes, Paisley, UK). For the identification of focal adhesions, a staining kit (Millipore, Nottingham, UK) was used. Actin filament and nuclear staining was performed with rhodamine-phalloidin (Molecular Probes, Life Technologies) and DAPI (Molecular Probes, Life Technologies) at recommended working concentrations. For western blotting, proteins (40 μg) were separated by SDS–PAGE and transferred to nitrocellulose. Antibodies used were anti-GSK-3β, anti-phospho-GSK-3β (Ser9) (Cell Signaling, Danvers, MA, USA), anti-GSK-3$\alpha + \beta$ (phospho Y279 + Y216) (Abcam, Cambridge, UK) and secondary antibodies as per manufacturer instructions (Dako, Cambridgeshire, UK).

Live cell imaging. Cells in 500 μl of growth medium ± 20 mM LiCl or 5 μM BIO were placed in each quarter of an Ibidi imaging dish (Nikon, Düsseldorf, Germany) and cultured in the incubation/imaging chamber of the Nikon Biostation IM time lapse imaging system. Cells were imaged for 24 h at 3-min intervals at 37 °C with 5% CO_2 in air. The Biostation IM associated software was used to create movie files for analysis. Cell tracking was performed in Image J with MTrackJ (www.imagescience.org/meijering/software/mtrackj/). For tracking, the nucleus of each cell was identified and tracked over 24 h at 150 min intervals.

Cell viability and proliferation analysis. Cell viability of both monolayers and spheroid aggregates incubated with growth medium ± GSK-3 inhibitors were measured using the WST-1

assay (Roche, West Sussex, UK) in 96 well plates, according to the manufacturer's recommendations. Tumour spheroids were imaged at 24 h, 48 h and 72 h using the EVOS cell imaging system and spheroid core area was calculated using Image J software to evaluate proliferation over time.

Statistical analysis. Statistical analysis was carried out using SPSS version 21 (IBM, New York, NY, USA). Statistical significance between multiple groups was determined by ANOVA. *P*-values <0.05 were considered statistically significant.

RESULTS

Paediatric glioma cell lines form tumour spheroids displaying different patterns of migration. In this study, we sought to identify chemotherapeutic agents capable of impairing migration and invasion in pHGG and DIPG cell lines. Tumour spheroids represent a useful model for examining tumour biology *in vitro* as they are three dimensional and comprise of a surface with ready access to nutrients and oxygen and an inner hypoxic core (Nowicki *et al*, 2008). Moreover, once embedded in a matrix such as collagen, cells can migrate outward from the core representing a model of the process of invasion (Nowicki *et al*, 2008).

Two pHGG cell lines, SF188 (glioblastoma) and KNS42 (glioblastoma) and one patient-derived DIPG cell line, HSJD-DIPG-007, were first examined for their ability to form spheroids in culture. Similar to Vinci *et al* (2012), we noted that all three cell lines readily formed round dense spheroids within 24 h when cultured in low adherence 96-well round bottomed plates (Figure 1A). Paediatric glioma tumour spheroids were then embedded in collagen, and cell migration was monitored over 72 h by light microscopy. The cell lines exhibited distinct migratory characteristics and migration patterns were strikingly different (Figure 1B): SF188 displayed a cogwheel pattern of migration with what appeared to be long thin symmetrical protrusions branching from the central core, whereas KNS42 and HSJD-DIPG-007 migrated by extending flattened protrusions and spreading in a sheet-like manner. The observed differences were also reflected in the migration indices obtained for the migration edge for each cell; KNS42 migrated significantly less than SF188 and HSJD-DIPG-007 (migration index 0.59). No significant difference was observed between the migration index of SF188 (0.87) and HSJD-DIPG-007 (0.78) (Figure 1C).

LiCl and BIO inhibit migration and invasion of paediatric glioma cells in 3D spheroid assays. The small molecule GSK-3 inhibitors, LiCl and the indirubin derivative BIO, have recently been shown to block migration in adult glioblastoma cell lines (Nowicki *et al*, 2008; Williams *et al*, 2011). Moreover, indirubin derivatives extend survival in animal glioblastoma orthotopic xenograft models and block metastasis *in vivo* (Williams *et al*, 2011). However, whether these agents exert similar effects upon migration and invasion in pHGG and DIPG cell lines has not been previously determined. In order to answer this question, tumour spheres from each cell line were embedded in collagen, overlaid

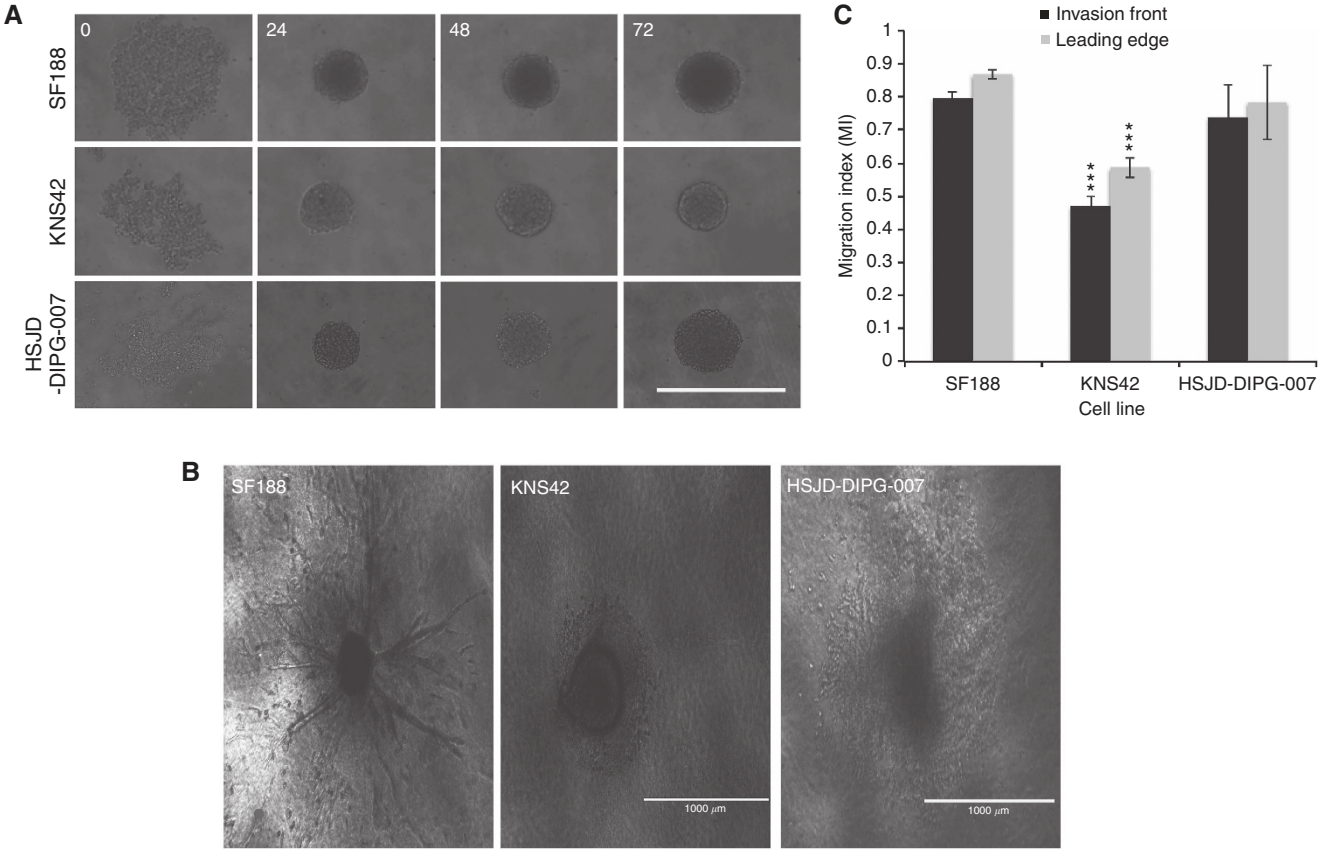

Figure 1. Paediatric glioma cell lines readily form tumour spheres from monolayers and demonstrate different patterns of migration. (**A**) The paediatric glioblastoma cell lines SF188 and KNS42 and the patient-derived DIPG cell line HSJD-DIPG-007 were evaluated for their ability to form tumour spheres in low adherent 96 well round-bottomed plates. After 72 h of incubation, all three cell lines formed tumour spheres. Images at $\times 100$ magnification. (**B**) SF188, KNS42 and HSJD-DIPG-007 tumour spheroids were capable of migrating after embedding in a collagen matrix as demonstrated at time point 72 h. Images at $\times 40$ magnification, scale bar $= 1000\,\mu$m. (**C**) The paediatric glioma cell lines differed in their ability to migrate as determined by the migration index (MI) for the invasion front and the leading edge. Error bars expressed as $\pm$ s.e.m. ***$P<0.001$ by T test. Results are representative of $n=3$ individual experiments.

with the drugs at varying concentrations and migration and invasion were imaged over 72 h (Figure 2A and B). A migration index was then calculated for each condition to compare the invasion front and leading edge zone for each treatment (Figure 2C).

We found that LiCl and BIO reduced migration and invasion in a concentration-dependent manner (Figure 2C). After 72 h, 10 or 5 μM BIO significantly blocked invasion of both pHGG cell lines (Figure 2C) (mean ± s.e.m. SF188 leading edge; control medium 0.869 ± 0.014, BIO 10 μM 0.292 ± 0.069 $P<0.001$, BIO 5 μM

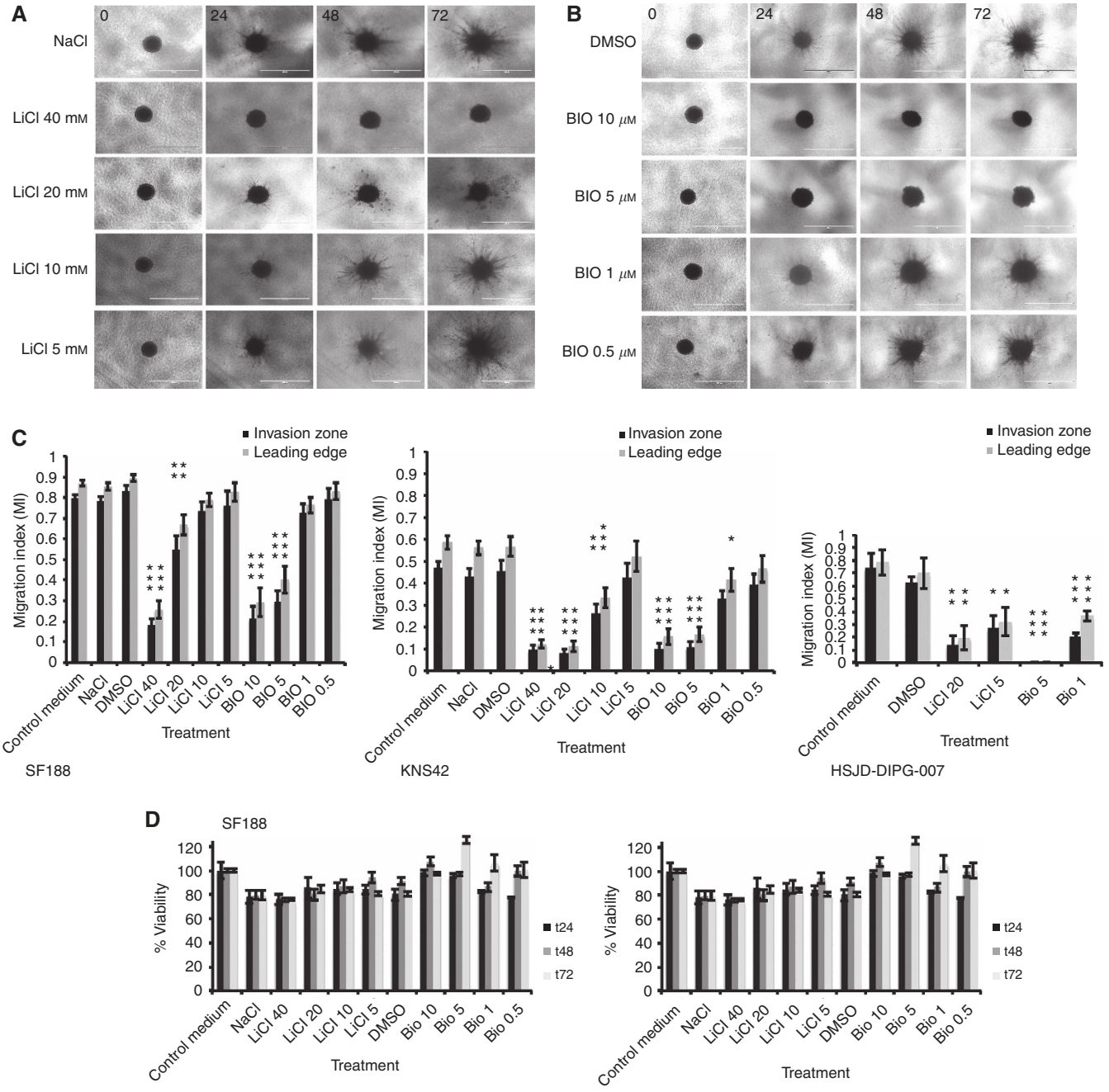

Figure 2. Inhibition of paediatric glioma tumour sphere invasion by LiCl and BIO. Tumour spheroids (SF188) were embedded in collagen and incubated in (**A**) LiCl at 40, 20, 10, 5 mM in NaCl or (**B**) BIO at 10, 5, 1, 0.5 μM in DMSO for 72 h. Migration was inhibited by both LiCl and BIO as shown in representative stills at 24, 48 and 72 h using the EVOS cell imaging system at ×40 magnification. Scale bar = 1000 μm. (**C**) Quantitative analysis of migration inhibition confirmed the results visualised by microscopy. Control medium used was Dulbecco's Modified Eagles' medium plus 10% heat-inactivated foetal calf serum. Both LiCl and BIO had statistically significant anti-migratory effects on the invasion zone and leading edge as indicated by * on all three cell lines (SF188, KNS42 and HSJD-DIPG-007). Results are representative of $n=3$ individual experiments. Error bars expressed as ± s.e.m. *$P<0.05$, **$P<0.01$, ***$P<0.001$ by ANOVA for each cell type and treatment. (**D**) Cell viability of paediatric glioma lines (SF188 and KNS42) grown as tumour spheroids treated with various concentrations of LiCl and BIO was determined by WST-1 assay and then expressed as a percentage of controls. Error bars expressed as ± s.e.m. The effects of LiCl and BIO on β-catenin localisation were evaluated for SF188 (**E**) and KNS42 (**F**) compared with medium mock-treated controls by immunofluorescent labelling. Arrows indicate β-catenin localisation. Red labelling–β-catenin, green labeling–actin, blue labeling–DAPI staining. Magnification ×63.

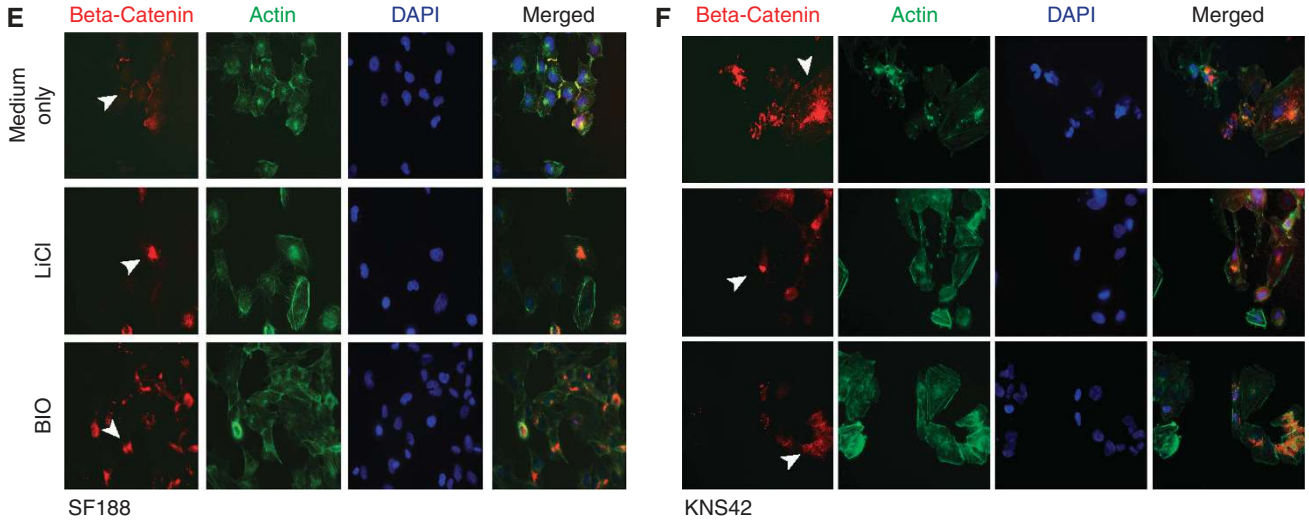

Figure 2. (Continued)

0.401 ± 0.065 $P<0.001$ KNS42 leading edge; control medium 0.587 ± 0.31, BIO 10 μM 0.157 ± 0.036 $P<0.001$, BIO 5 μM 0.166 ± 0.033 $P<0.001$). The invasion of the DIPG cell line at 72 h was significantly blocked by BIO at both 5 and 1 μM (mean ± s.e.m. HSJD-DIPG-007 leading edge; control medium 0.784 ± 0.1, BIO 5 μM 0.0 $P<0.001$, BIO 1 μM 0.36 ± 0.040 $P<0.001$). Treatment with 40 and 20 mM LiCl for 72 h also caused a statistically significant reduction of invasion for SF188 and KNS42 (for both the invasion front and leading edge (Figure 2C)) (mean ± s.e.m. SF188 leading edge; control medium 0.869 ± 0.014, LiCl 40 mM 0.256 ± 0.042 $P<0.001$, LiCl 20 mM 0.667 ± 0.05 $P=0.005$, KNS42 control medium 0.587 ± 0.31, LiCl 40 mM 0.123 ± 0.02 $P<0.001$, LiCl 20 mM 0.112 ± 0.026 $P<0.001$). LiCl at 20 mM and 5 mM significantly reduced the invasion of HSJD-DIPG-007 following 72 h of treatment (mean ± s.e.m. HSJD-DIPG-007 leading edge; control medium 0.784 ± 0.1, LiCl 20 mM 0.19 ± 0.92 $P<0.01$, LiCl 5 mM 0.322 ± 0.11 $P<0.05$).

To confirm that the observed effects on migration after drug treatment were the result of specific anti-migratory effects and not caused by non-specific cytotoxic or anti-proliferative effects, we investigated the effects of the two inhibitors on spheroid viability by WST-1 assays. This assay has previously been used to determine the viability of cells grown as spheroids (Van Beusechem *et al*, 2003). In the 3D spheroid system, both pHGG cell lines displayed viability of at least 75% or above for all treatments with LiCl and BIO (Figure 2D). Proliferation, as determined by spheroid core size changed over time, was only reduced at 40 mM LiCl in SF188 (Supplementary Figure 2).

The effect of LiCl and BIO on migration has previously been investigated in adult glioma and their anti-migratory activity has been attributed to their ability to inhibit GSK-3 and stabilise β-catenin (Nowicki *et al*, 2008; Williams *et al*, 2011). In order to confirm that LiCl and BIO target GSK-3 in pHGG, we carried out western blot analysis of the activated and inactivated forms of GSK-3 protein. LiCl increased Ser9 phosphorylated GSK-3β (inactivated form) and BIO decreased the activating tyrosine of GSK-3$\alpha\beta$ (Supplementary Figure 3). Next, we examined β-catenin localisation and staining by IF post treatment (Figure 2E and F). For SF188, cells treated with both LiCl or BIO displayed reduced staining of β-catenin at the plasma membrane with enhanced cytoplasmic and peri-nuclear staining. This was more marked for cells treated with BIO than LiCl (Figure 2E). For KNS42, surface and intracellular staining of β-catenin was observed in the control; however, BIO and LiCl treatment resulted in internalisation of β-catenin, which was more pronounced for BIO treatment (Figure 2F).

Migration of paediatric HGG cells in transwell assays is inhibited after treatment with LiCl and BIO. In order to confirm the anti-migratory effects of LiCl and BIO observed in the spheroid model, a 2D transwell assay was performed. Both pHGG cell lines were able to migrate through the transwell membranes, with SF188 demonstrating the most migration over 4 h (data not shown). In the transwell experiments, treatment with 20 mM LiCl and 5μM BIO reduced cell migration in both SF188 and KNS42 confirming the results obtained from the spheroid assays (Figure 3A). Five micromoles of BIO reduced migration in both pHGG cell lines and reached statistical significance for KNS42. Treatment with 20 mM LiCl also reduced migration in both cell lines and reached statistical significance for SF188. We conclude that at concentrations of 20 mM and 5 μM respectively, LiCl and BIO have significant anti-migratory effects on pHGG cells. Consequently, all subsequent migration assays and IF studies were performed on cells treated with LiCl or BIO at these concentrations. Additionally, at the same highest concentrations of NaCl or DMSO, no adverse effects on cell biology were observed; thus, we carried out all subsequent experiments using growth medium (Dulbecco's Modified Eagles' medium plus 10% heat-inactivated foetal calf serum) as the control.

Next, we assessed the effect of LiCl and BIO treatment on cell monolayer viability via a WST-1 assay over a time course of 72 h (Figure 3B). SF188 was the most sensitive cell line to both treatments. At 24 h, which would most closely correlate to the time scale for the transwell assay, both cell lines demonstrated greater than 80% viability when treated with LiCl. SF188 was more sensitive to 10 μM BIO at 24 h, with cell viability at 57%; however, KNS42 was resistant to the effects of BIO with greater than 90% cell viability demonstrated at 24 h. Over 72 h, when cultured as monolayers, both pHGG cell lines exhibited increased sensitivity to LiCl and BIO treatment compared with spheroid cultures. This is unsurprising because 3D aggregates of tumour cells, including pHGG cells, have been shown to be generally more drug resistant than 2D cultures (Mehta *et al*, 2012; Smith *et al*, 2012). Finally, to demonstrate that LiCl and BIO are not directly cytotoxic at concentrations of 20 mM and 5 μM respectively, monolayers of both pHGG cell lines were imaged by time lapse microscopy following treatment with LiCl and BIO for 24 h. After 24 h, the drugs were removed, and both pHGG cell lines demonstrated recovery and resumed their normal morphology (results not shown).

LiCl and BIO inhibit paediatric HGG cell migration on a topographic nanofibre-based migration assay. A nanofibre-based

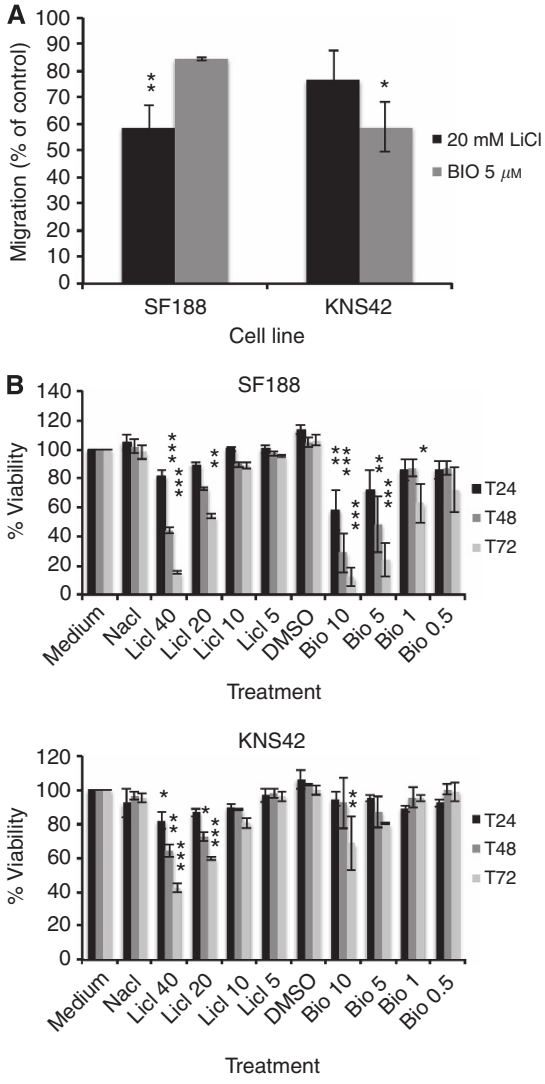

Figure 3. LiCl and BIO inhibit migration of pHGG cells in a 2D Transwell assay. (**A**) Cells pre-treated with either control medium, LiCl and BIO were assessed for their ability to migrate across a transwell membrane after 4 h incubation. At 20 mM LiCl or 5 μM BIO, inhibition of migration was observed in SF188 and KNS42. Results are representative of $n=3$ individual experiments. Error bars are expressed as ± s.e.m. *$P<0.05$, **$P<0.01$ by ANOVA for each cell type and treatment. (**B**) The effect of LiCl and BIO at various concentrations on the paediatric glioma lines (SF188 and KNS42) grown as monolayers was assessed by a WST-1 assay and was expressed as a percentage of controls. Results are representative of $n=3$ individual experiments. Error bars expressed as ± s.e.m. *$P<0.05$, **$P<0.01$, ***$P<0.001$ by ANOVA for each cell type and treatment.

assay was also used to assess the effect of GSK-3 inhibition on migration of pHGG cell lines on a 3D scaffold. This assay utilises aligned fibres of polycaprolactone to stimulate cell migration via topographic cues (Johnson *et al*, 2009). When cells are plated on the nanofibre scaffold they adhere, elongate and move along the fibre axis (Figure 4A).

Firstly, we noted that each pHGG cell line was able to migrate in this model system and further confirmation of the anti-migratory effect of the GSK-3 inhibitors LiCl and BIO was obtained. As seen in previous assays, SF188 was the most migratory cell line in terms of distance travelled. Perimeter indices (% increase from the spheroid perimeter to the perimeter marking the migrated cells) were calculated for each cell line. Treatment with LiCl and BIO decreased the migration index (Figure 4B) and perimeter index (Figure 4C) for both pHGG cell lines when compared with controls. However, the effect was more marked for KNS42 when compared with SF188.

Live cell imaging of paediatric HGG cell line migration. Given the accumulation of evidence that LiCl and BIO are able to reduce the migration of SF188 and KNS42 cells, we went on to hypothesise that we should be able to detect direct changes in cell morphology and motility following treatment. We investigated the effects of LiCl and BIO on individual cell morphology by live cell imaging over 24 h. SF188 and KNS42 cells were incubated with 20 mM LiCl, 5 μM BIO or control medium and time lapse imaging was performed for 24 h (Figure 5A and B). In terms of motility, SF188 cells were more motile and demonstrated greater velocity than KNS42 cells (mean ± s.e.m. velocity SF188 control $0.295 \pm 0.0018\ \mu m\ min^{-1}$ KNS42 control $0.0599 \pm 0.0048\ \mu m\ min^{-1}$) (Figure 5C–E). Cells from both lines were able to polarise under normal conditions; however, treatment with 20 mM LiCl and 5 μM BIO reduced polarity as demonstrated by a reduction in displacement, but this did not reach statistical significance (displacement SF188 control 176.5 ± 74.6, LiCl 20 mM 52.5 ± 15.3, BIO 5 μmol 107.2 ± 61.7, KNS42 control 28.6 ± 8.23, LiCl 20 mM 14.7 ± 2.35, BIO 5 μmol 14.19 ± 1.9). Twenty millimoles of LiCl and 5 μM BIO reduced the velocity of SF188 cells (control $0.295 \pm 0.0018\ \mu m\ min^{-1}$, LiCl 20 mM $0.153 \pm 0.047\ \mu m\ min^{-1}$ $P=0.049$, BIO 5 μmol $0.21 \pm 0.041\ \mu m\ min^{-1}$ $P=0.247$) whereas treatment only with 5 μM BIO reduced the velocity of KNS42 cells (control $0.0599 \pm 0.0048\ \mu m\ min^{-1}$, LiCl 20 mM $0.0761 \pm 0.0063\ \mu m\ min^{-1}$ $P=0.98$, BIO 5 μmol $0.0501 \pm 0.041\ \mu m\ min^{-1}$ $P=0.345$). LiCl and BIO appeared to have a greater effect on the polarity of KNS42 cells than velocity. Apart from the effects on cell motility, both LiCl and BIO appeared to affect cell morphology with cells rounding up after treatment and demonstrating loss of polarity and blebbing (Figure 5A and B). Non-apoptotic plasma membrane blebbing has been implicated in cell movement, mode of migration and disruption of actin-membrane interactions (Fackler and Grosse, 2008). Taken together, these observations may explain why the cells incubated with these drugs demonstrated a reduction in migration in the previous experiments.

Immunofluorescence studies reveal differences in cellular morphology in paediatric HGG cell lines and morphological changes after drug treatment. We next utilised IF techniques to investigate the effects of the GSK-3 inhibitors on the microtubule cytoskeleton (polarity), actin cytoskeleton (morphology, motility) and focal adhesions (cell motility, morphology). Both cell lines were characterised by distinctive microtubule network, actin cytoskeleton and focal adhesion staining patterns. Immunofluorescence labelling revealed either elaborate microtubule networks across the whole cell body or a more pronounced cell surface localisation, whereas for actin we observed stress fibres, cortical actin or a diffuse internal localisation ('other') and whole body, cortical or diffuse focal adhesion labelling, which changed in response to treatment. Untreated SF188 cells appeared as large cells with a microtubule network, pronounced actin stress fibres and focal adhesions across the whole cell body (Figure 6A). After treatment with 20 mM LiCl and 5 μM BIO, we observed that the cells appeared more rounded with pronounced microtubule localisation on the cell surface. Actin stress fibre labelling in the control cells was marked and decreased in the cells treated with LiCl and BIO with a more diffuse cortical and internal actin distribution ('other'). (Figure 6C). Focal adhesions across the cell body were diminished after treatment with the inhibitors and, when present, re-distributed to the surface of the cells (Figure 6D). KNS42 cells appeared as medium-sized elongated cells with a microtubule network and had diffuse actin stress fibres (Figure 6B).

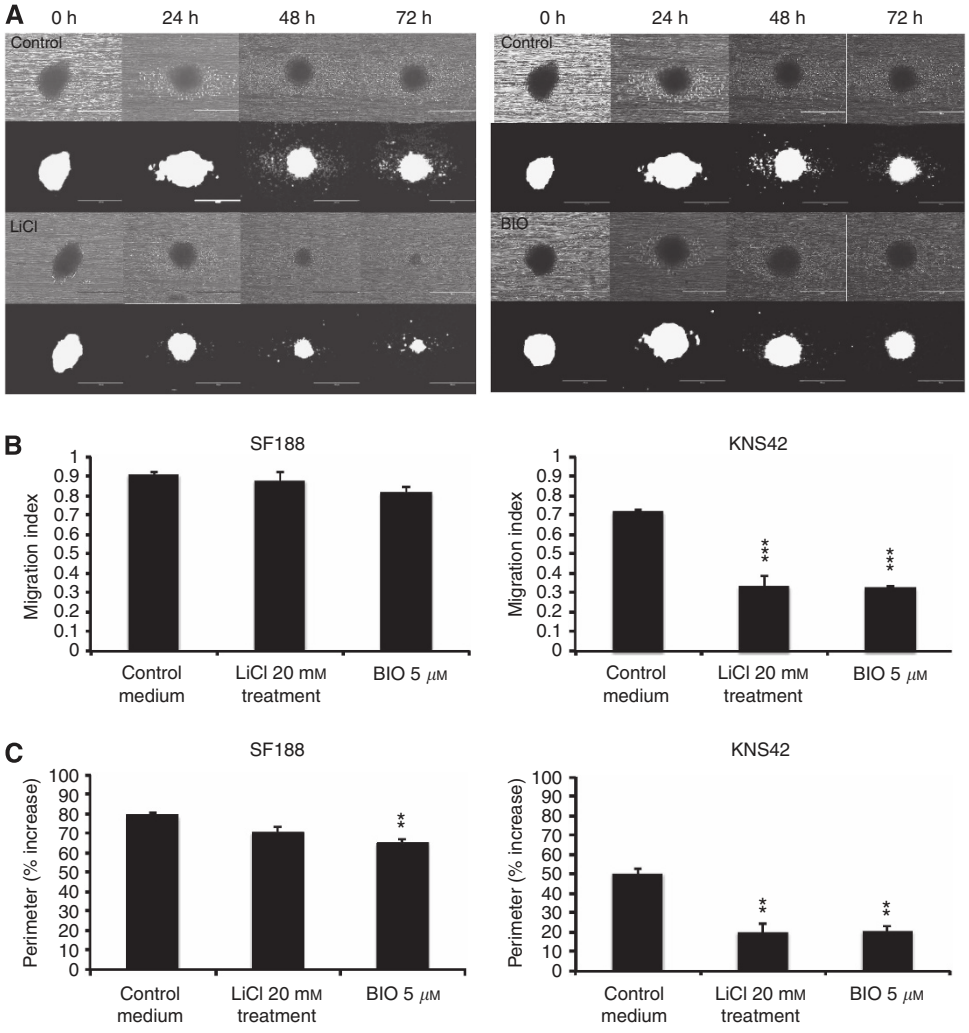

Figure 4. LiCl and BIO reduce migration of pHGG cells in an aligned nanofibre 3D migration assay. Tumour cell aggregates formed from hanging drops and labelled with a fluorescent cell tracker were placed in wells containing aligned poly-ε-caprolactone fibres and cultured ± 20 mM LiCl or 5 μM BIO. Migration was recorded either as phase contrast or fluorescent images for quantification. (**A**) Spheroids formed from cell line SF188 migrated along the nanofibre as evidenced by phase contrast and fluorescent imaging; the addition of LiCl or BIO had a marked anti-migratory effect on the cells. Images at × 40 magnification. Scale bar = 400 μm. (**B**) Quantification and comparison of the effects of 20 mM LiCl and 5 μM BIO on the migration index for both cell lines. Results representative of at least three repeats. Error bars are expressed as ± s.e.m. *$P<0.05$, **$P<0.01$, ***$P<0.001$ by ANOVA for each cell type and treatment. (**C**) Quantification and comparison of the effects of 20 mM LiCl and 5 μM BIO on the perimeter index for both cell lines. Error bars are expressed as ± s.e.m. *$P<0.05$, **$P<0.01$, ***$P<0.001$ by ANOVA for each cell type and treatment.

Focal adhesions appeared to be associated with actin filaments in untreated cells. After addition of the inhibitors, the cells rounded up and were smaller in comparison to the untreated cells. The microtubule network was still present, however, actin stress fibres appeared to be less pronounced (especially after treatment with BIO) (Figure 6C) and focal adhesions co-localised diffusely with the actin filament and when present relocated to the cortex (Figure 6D).

DISCUSSION

Paediatric high grade glioma and DIPG are devastating tumours associated with poor prognosis and despite attempts at aggressive therapy, tumours inevitably recur owing to their diffuse and invasive nature. As a result, there is a need to identify and develop novel therapeutic approaches that target and block tumour invasion. In this study, we characterised the migratory behaviour of two pHGG cell lines and one patient-derived DIPG cell line in 2D and 3D models and investigated their response to GSK-3 inhibitors. We have shown that different paediatric glioma cell lines are able to grow as tumour spheroids, which are capable of migrating through a collagen matrix. To the best of our knowledge, this is the first time that DIPG migration has been described using a 3D model. Each cell line investigated demonstrated a unique pattern of migration and invasion. We also examined the motility of individual pHGG cells via live cell imaging, which indicated different speeds and morphology in two cell lines. In addition, we have demonstrated for the first time that LiCl and BIO, which have anti-invasive effects in adult glioma cell lines (Nowicki *et al*, 2008; Williams *et al*, 2011), also inhibit the migration of paediatric glioma cells in 2D (transwell) and 3D (spheroid invasion assay and nanofibre plates) assays. We observed a significant inhibition of migration with 5 μM BIO and 20 mM LiCl in all of our paediatric glioma cell lines. This was not accompanied by marked loss of viability when SF188 and KNS42 cells were cultured as multicellular spheroids. Our data correlate with previously published results for these inhibitors in adult glioma models (Nowicki *et al*,

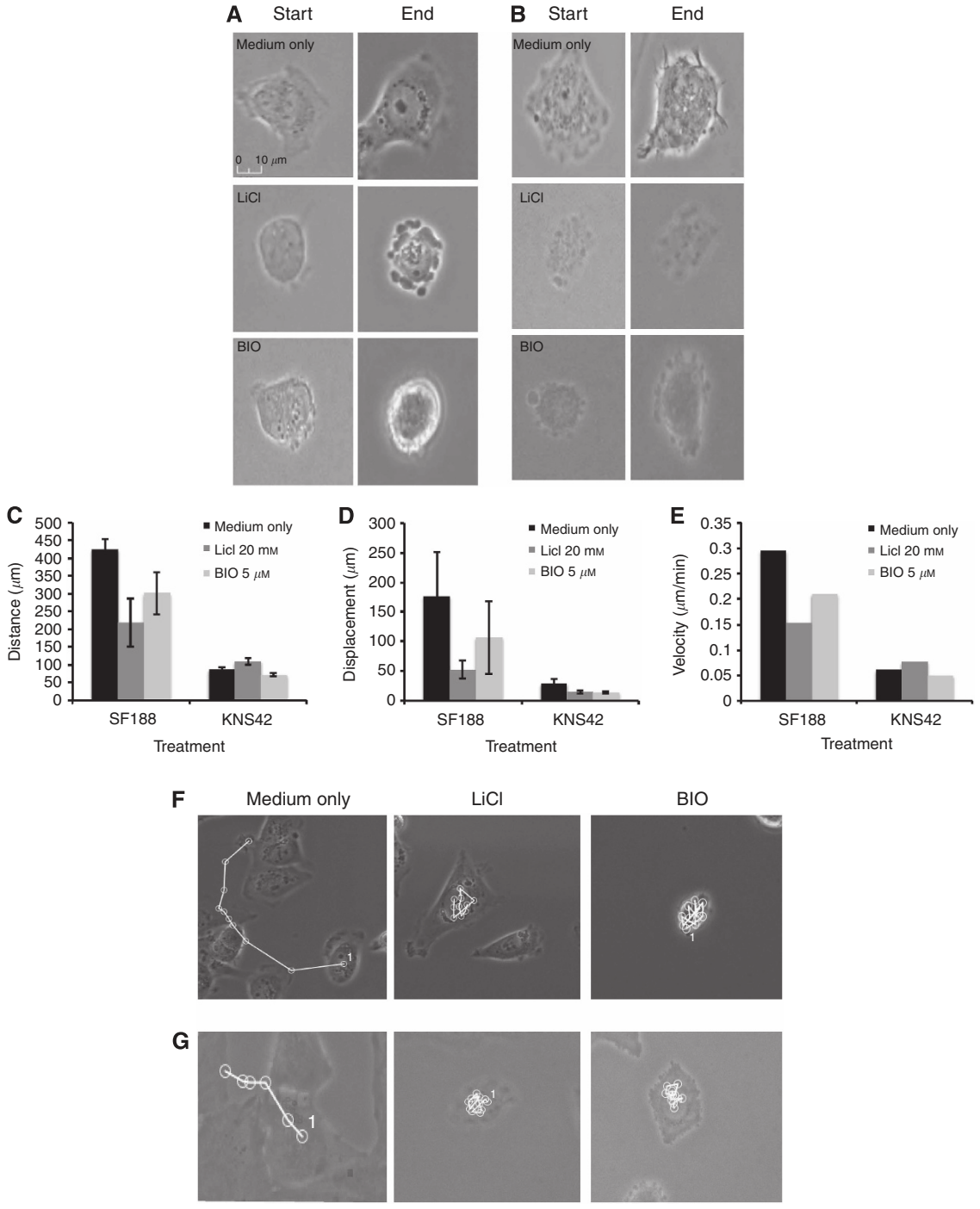

Figure 5. Live cell imaging of pHGG cell lines reveals differences in migration velocity alongside changes in polarity and morphological appearance following treatment with LiCl and BIO. Paediatric glioma cell lines SF188 and KNS42 were incubated with 20 mM LiCl, 5 μM BIO or growth medium and time lapse imaging was performed for 24 h using the Nikon Biostation IM time lapse imaging system. Stills taken at time 0 h and 24 h from movies of SF188 (**A**) and KNS42 (**B**) treated with either 20 mM LiCl, 5 μM BIO or growth medium demonstrate changes in the morphological appearance of individual cells following treatment. Quantification analysis of distance (**C**) displacement (**D**) and velocity (**E**) from live cell imaging of both cell lines following treatment with 20 mM LiCl or 5 μM BIO. Error bars are expressed as ± s.e.m. *$P<0.05$ by ANOVA for each cell type and treatment. Tracking analysis of SF188 (**F**) and KNS42 (**G**) from live cell imaging following treatment with 20 mM LiCl or 5 μM BIO demonstrates differences in motility between cell lines and treatments.

2008; Williams *et al*, 2011). Finally, we have shown that LiCl and BIO treatment altered the motility of individual pHGG cells, resulting in overall reduced movement, loss of polarity and cell rounding. This observation is novel and demonstrates the specific effects of LiCl and BIO on cell morphology and motility. Overall, our study is amongst the very few to have identified existing clinical and preclinical agents, which are capable of disrupting migration and invasion in pHGG and DIPG cell lines.

Cell migration may be achieved by a set of component processes, which are often regulated by the same effectors regardless of the cell type and the mode of migration. Broadly, these processes are based on polarisation, protrusion and adhesion,

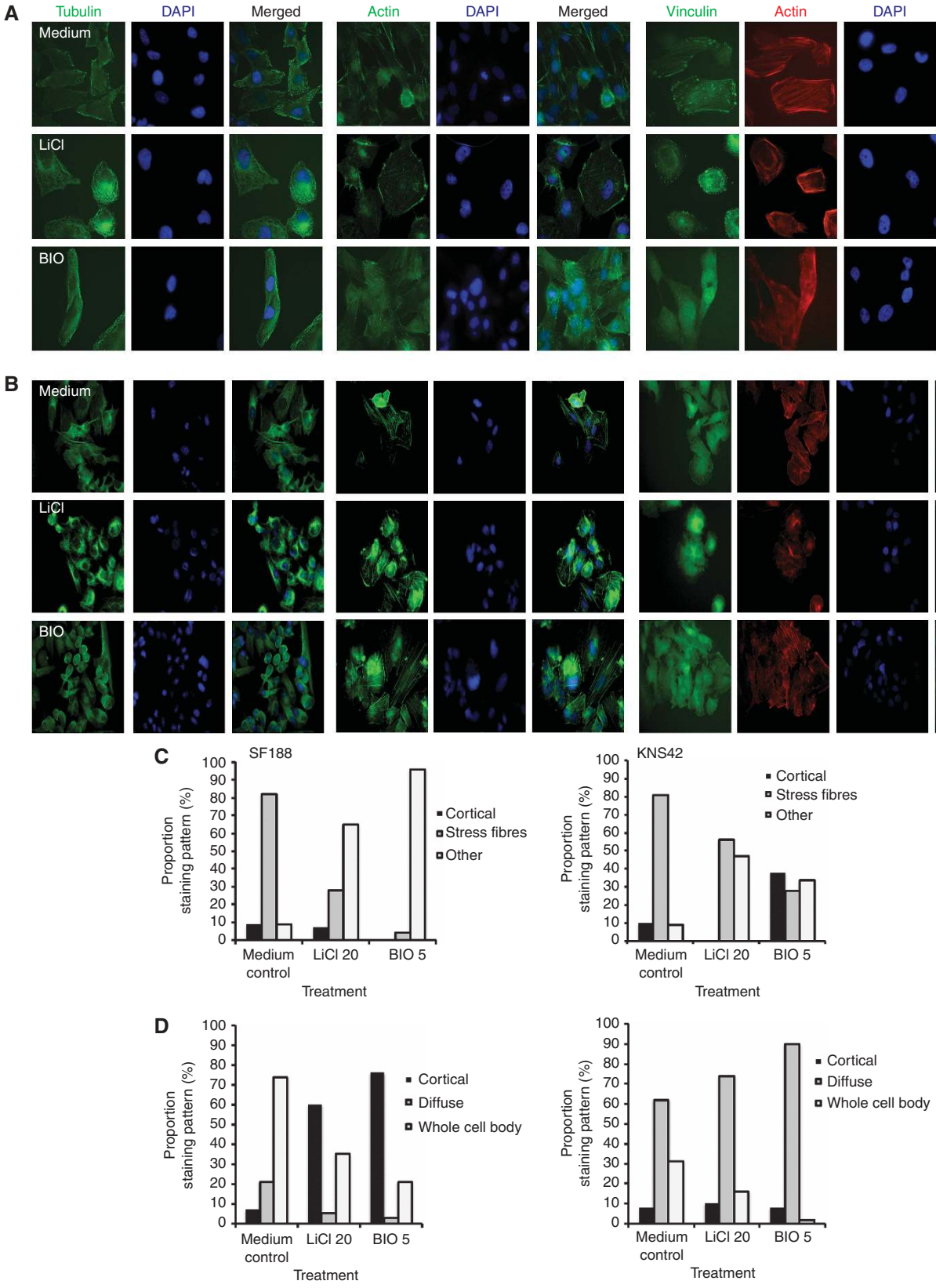

Figure 6. Immunofluorescence studies reveal cytoskeletal changes in two pHGG cell lines after LiCl and BIO treatment. The effects of the two inhibitors LiCl and BIO on cell morphology of (**A**) SF188 and (**B**) KNS42 were assessed by immunofluorescent labelling. Green labelling–alpha-tubulin, actin or vinculin; red labelling–actin and blue labelling–DAPI staining. Magnification $\times 63$; changes in the distribution of (**C**) the actin cytoskeleton (cortical, stress fibres, 'other') and (**D**) focal adhesions (cortical, diffuse, whole cell body) were observed following scoring of at least 100 cells.

translocation of the cell body and retraction of the rear. They are also coordinated and integrated by extensive transient signalling networks (Wehrle-Haller and Imhof, 2003). We therefore investigated the effect of LiCl and BIO on the interaction between the microtubule cytoskeleton, actin skeleton and focal adhesions on two established pHGG cell lines that grow as monolayers. In both pHGG cell lines examined, we observed that microtubules re-localised to the surface of cells. There was a change in the actin cytoskeleton with re-localisation of the actin fibres to the cell periphery and we also noted a change in focal adhesion point turn over and dynamics with a marked re-distribution of focal adhesion points to the cell surface or apparent loss of focal adhesion foci. The cells appeared to be immobilised in response to the loss of polarity, motility and attachment-detachment dynamics, accounting for their inability to migrate.

One postulated mechanism for the anti-migratory effects of LiCl and BIO is through GSK-3 inhibition. Glycogen synthase kinase-3 is thought to be involved in the control of cell migration, through its role in regulating cellular structure alongside microtubule and focal adhesion dynamics (Grimes and Jope, 2001; Sun *et al*, 2009). In adult HGG, the effect of LiCl and BIO on migration has previously been investigated and their anti-migratory activity has been attributed to their ability to inhibit GSK-3 and stabilise β-catenin via the canonical Wnt signalling pathway (Luo, 2009). In adult glioma models, LiCl has been shown to increase β-catenin reporter activity and β-catenin knockdown has been demonstrated to rescue the anti-migratory effects of BIO (Nowicki *et al*, 2008; Williams *et al*, 2011). In our study, we examined β-catenin localisation by IF post treatment of pHGG cells with LiCl and BIO, and observed a marked internalisation of β-catenin to the cytoplasm and nucleus following treatment. This observation has also been noted in adult glioma following LiCl and BIO treatment (Williams, 2011) and provides evidence to support the effectiveness of LiCl and BIO as an inhibitor of GSK-3. Furthermore, western blot analysis of our pHGG lines confirmed that LiCl increased Ser9 phosphorylated GSK-3β (inactivated form) and BIO decreased the activating tyrosine of GSK-3$\alpha\beta$.

Both LiCl and BIO have potential for clinical application. LiCl has been used to treat psychiatric conditions such as bipolar disorder for many decades (Mitchell, 1999) and BIO is part of the family of indirubins, which have been identified as the active ingredient of the Chinese medicine Danggui Longhui Wan, which has anti-leukemic activity (Hoessel *et al*, 1999). Other GSK-3 inhibitors have been developed and tested in a variety of preclinical studies (Meijer *et al*, 2004; Eldar-Finkelman and Martinez, 2011), however, current hurdles for the use of such drugs in clinical practice include optimisation of drug delivery and avoidance of toxic systemic accumulation of the drug. In particular, LiCl has a narrow therapeutic window, inducing nephrotoxicity at concentrations greater than 1.5 mM *in vivo* (Nowicki *et al*, 2008). Although our data detect significant anti-migratory effects on paediatric glioma at concentrations as low as 5 mM, alternative methods of drug delivery such as convection-enhanced delivery or local delivery with polymers may be required to attain localised high concentrations of the drug in human brain tumours (Nowicki *et al*, 2008; Siegal, 2013) and this requires further evaluation *in vivo* with preclinical models. Alternatively, the development of specific novel GSK-3 inhibitors capable of crossing the blood–brain barrier at concentrations associated with clinically acceptable side effect profiles will help overcome this problem. Finally, owing to the lack of published mouse models of paediatric glioma invasion, we have not been able to address the anti-migratory effects of GSK-3 inhibitors *in vivo*. Studies of adult glioma have shown that GSK-3 inhibitors of the indirubin family are able to reduce invasion of glioma cells *in vivo* (Williams *et al*, 2011) and development of a paediatric orthotopic xenograft model of migration to test novel GSK-3 inhibitors forms a major part of our ongoing studies in this area.

In summary, we have characterised the migratory behaviour of paediatric glioma cell lines in 2D and 3D models and conclude that GSK-3 inhibitors, such as LiCl and BIO, may be novel candidates for migration inhibition in pHGG and DIPG and as such warrant further investigation as therapeutics for this challenging group of tumours.

ACKNOWLEDGEMENTS

We would like to thank our funders Yorkshire Cancer Research, the PPR Foundation, Candlelighters Children Cancer Charity and Brain Tumour Research and Support across Yorkshire who have helped support this work.

CONFLICT OF INTEREST

The authors declare no conflict of interest.

REFERENCES

Agudelo-Garcia PA, De Jesus JK, Williams SP, Nowicki MO, Chiocca EA, Liyanarachchi S, Li PK, Lannutti JJ, Johnson JK, Lawler SE, Viapiano MS (2011) Glioma cell migration on three-dimensional nanofiber scaffolds is regulated by substrate topography and abolished by inhibition of STAT3 signaling. *Neoplasia* **13**: 831–840.

Broniscer A, Gajjar A (2004) Supratentorial high-grade astrocytoma and diffuse brainstem glioma: two challenges for the pediatric oncologist. *Oncologist* **9**: 197–206.

Del Duca D, Werbowetski T, Del Maestro RF (2004) Spheroid preparation from hanging drops: characterization of a model of brain tumor invasion. *J Neurooncol* **67**: 295–303.

Demuth T, Berens ME (2004) Molecular mechanisms of glioma cell migration and invasion. *J Neurooncol* **70**: 217–228.

Eldar-Finkelman H, Martinez A (2011) GSK-3 inhibitors: preclinical and clinical focus on CNS. *Front Mol Neurosci* **4**: 32.

Fackler OT, Grosse R (2008) Cell motility through plasma membrane blebbing. *J Cell Biol* **181**: 879–884.

Grimes CA, Jope RS (2001) The multifaceted roles of glycogen synthase kinase 3beta in cellular signaling. *Prog Neurobiol* **65**: 391–426.

Hoessel R, Leclerc S, Endicott JA, Nobel ME, Lawrie A, Tunnah P, Leost M, Damiens E, Marie D, Marko D, Niederberger E, Tang W, Eisenbrand G, Meijer L (1999) Indirubin, the active constituent of a Chinese antileukaemia medicine, inhibits cyclin-dependent kinases. *Nat Cell Biol* **1**: 60–67.

Johnson J, Nowicki MO, Lee CH, Chiocca EA, Viapiano MS, Lawler SE, Lannutti JJ (2009) Quantitative analysis of complex glioma cell migration on electrospun polycaprolactone using time-lapse microscopy. *Tissue Eng Part C Methods* **15**: 531–540.

Jones C, Perryman L, Hargrave D (2012) Paediatric and adult malignant glioma: close relatives or distant cousins? *Nat Rev Clin Oncol* **9**: 400–413.

Louis DN (2006) Molecular pathology of malignant gliomas. *Annu Rev Pathol* **1**: 97–117.

Luo J (2009) Glycogen synthase kinase 3beta (GSK3beta) in tumorigenesis and cancer chemotherapy. *Cancer Lett* **273**: 194–200.

Ma XH, Piao S, Wang D, McAfee QW, Nathanson KL, Lum JJ, Li LZ, Amaravadi RK (2011) Measurements of tumor cell autophagy predict invasiveness, resistance to chemotherapy, and survival in melanoma. *Clin Cancer Res* **17**: 3478–3489.

Mehta G, Hsiao AY, Ingram M, Luker GD, Takayama S (2012) Opportunities and challenges for use of tumor spheroids as models to test drug delivery and efficacy. *J Control Release* **164**: 192–204.

Meijer L, Flajolet M, Greengard P (2004) Pharmacological inhibitors of glycogen synthase kinase 3. *Trends Pharmacol Sci* **25**: 471–480.

Mitchell PB (1999) On the 50th anniversary of John Cade's discovery of the anti-manic effect of lithium. *Aust N Z J Psychiatry* **33**: 623–628.

Nowicki MO, Dmitrieva N, Stein AM, Cutter JL, Godlewski J, Saeki Y, Nita M, Berens ME, Sander LM, Newton HB, Chiocca EA, Lawler S (2008) Lithium

inhibits invasion of glioma cells; possible involvement of glycogen synthase kinase-3. *Neuro Oncol* **10**: 690–699.
Siegal T (2013) Which drug or drug delivery system can change clinical practice for brain tumor therapy? *Neuro Oncol* **15**: 656–669.
Smith SJ, Wilson M, Ward JH, Rahman CV, Peet AC, Macarthur DC, Rose FR, Grundy RG, Rahman R (2012) Recapitulation of tumor heterogeneity and molecular signatures in a 3D brain cancer model with decreased sensitivity to histone deacetylase inhibition. *PLoS One* **7**: e52335.
Sun T, Rodriguez M, Kim L (2009) Glycogen synthase kinase 3 in the world of cell migration. *Dev Growth Differ* **51**: 735–742.
Van Beusechem VW, Mastenbroek DC, van den Doel PB, Lamfers ML, Grill J, Würdinger T, Haisma HJ, Pinedo HM, Gerritsen WR (2003) Conditionally replicative adenovirus expressing a targeting adapter molecule exhibits enhanced oncolytic potency on CAR-deficient tumors. *Gene Ther* **10**: 1982–1991.
Vinci M, Gowan S, Boxall F, Patterson L, Zimmermann M, Court W, Lomas C, Mendiola M, Hardisson D, Eccles SA (2012) Advances in establishment and analysis of three-dimensional tumor spheroid-based functional assays for target validation and drug evaluation. *BMC Biol* **10**: 29.
Wakefield JG, Stephens DJ, Tavaré JM (2003) A role for glycogen synthase kinase-3 in mitotic spindle dynamics and chromosome alignment. *J Cell Sci* **116**: 637–646.
Warren KE (2012) Diffuse intrinsic pontine glioma: poised for progress. *Front Oncol* **2**: 205.
Wehrle-Haller B, Imhof BA (2003) Actin, microtubules and focal adhesion dynamics during cell migration. *Int J Biochem Cell Biol* **35**: 39–50.
Williams SP (2011) *The role of glycogen synthase kinase in glioblastoma multiforme migration and invasion*. PhD thesis, The Ohio State University: Columbus, OH, USA.
Williams SP, Nowicki MO, Liu F, Press R, Godlewski J, Abdel-Rasoul M, Kaur B, Fernandez SA, Chiocca EA, Lawler SE (2011) Indirubins decrease glioma invasion by blocking migratory phenotypes in both the tumor and stromal endothelial cell compartments. *Cancer Res* **71**: 5374–5380.

Supplementary Information accompanies this paper on British Journal of Cancer website (http://www.nature.com/bjc)